N87-25273

MODELING AND IMPLEMENTATION OF WIND SHEAR DATA

Walter Frost
FWG Associates, Inc.
Tullahoma, Tennessee

The problems of implementing the JAWS wind shear data are discussed in this presentation. First of all, I will describe the data sets from the point of view of utilizing them in an aircraft performance computer program. Then I will describe some of the problems of non-standard procedures in terms of programming the equations of aircraft motion when the effects of temporal and spatially variable winds are included. Finally, I will show you some of the computed effects of the various wind shear terms.

The specific tasks to be performed under NCAR contract are listed in Figure 1. The collection and processing of the dual and triple Doppler returns have been described in references 1 and 2. The processing of the Doppler radar signals resolves the data into a rectangular array of three Cartesian velocity components. The array is updated every two minutes, resulting in the fourth dimension, time. Thus we have, essentially, blocks of data that represent every two minutes of the microburst phenomenon taking place.

Figure 2 illustrates the origin of the coordinate system used on the NCAR data tapes. The origin of the x,y,z coordinate system is located at CP-2. The x coordinate is measured positive toward the east; and the y coordinate is measured positive toward the north. The z coordinate is positive in the vertical direction upward. When implementing the wind data into the airplane equations of motion, one must be aware that the data are provided in an earth-fixed coordinate system.

At present, we have looked at three data sets. The primary data set we have looked at is the August 5 data set. It was measured in the region indicated in Figure 2. The numbers in parentheses are the x, y coordinates of the region in kilometers relative to CP-2. The June 29 data set also shown in Figure 2 is another data set that came out earlier. These data are not processed in exactly the same manner as the August 5 data and they may show more severe wind shear effects than are real. We want to caution you to not use this data set because all the smoothing techniques and mass balance verification procedures currently perfected by NCAR have not been applied to the June 29 data set. The July 14 data set was measured at the location indicated on Figure 2. A great deal of work with this data set has not yet been carried out. Never before have we measured velocity to the resolution achieved by JAWS in a volume of space that is, essentially, 12 km square and 2 km high. We have wind velocity entirely throughout this volume element. The data is provided to us on data tapes with an established grid system. The grid spacing for the August 5 case is 150 m in the horizontal direction (both lateral and longitudinal) and 250 m in the vertical direction (see Figure 3).

In the 12 km square by 2 km high volume element, there are 81 grid points on each side, plus 9 grid points in the vertical direction. One of the problems that scares everybody immediately when you look at this data set is that you have 81 by 81 by 9 grid points; and if you have three wind components at each grid point, you end up with approximately 177,000 data points. Storage capacity of a computer may thus begin to be

- Prepare from the JAWS data, four-dimensional computer models on microburst velocities as input for flight simulator models.

- Incorporate the new four-dimensional wind shear models into numerical computations to determine critical wind shear severity thresholds, access the scales of motion which lead to dangerous aircraft response, determine the relative importance of the horizontal versus the vertical wind speed component, define the test flight deterioration parameters, and evaluate operational procedures for use in wind shear encounters.

- Review flight simulator theories and aircraft equations of motion to assure compatibility of the wind shear models with existing simulator capabilities and computer storage capacity.

- Combine the instrumented aircraft high-frequency wind speed measurements with Doppler radar data to provide a meaningful turbulence model for addition to the wind shear simulation input models.

Figure 1. Objectives of current research

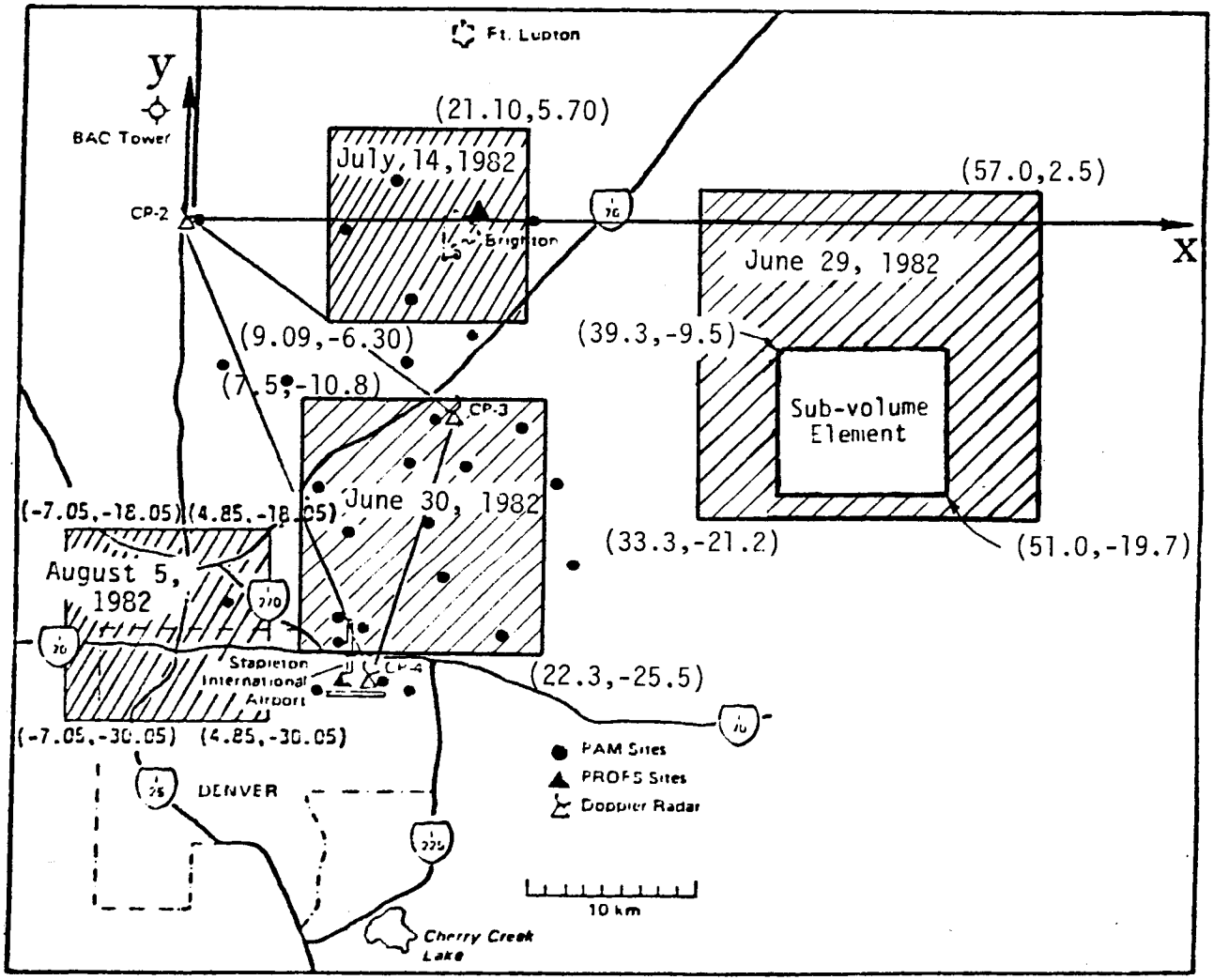

Figure 2. Location of Doppler CP-2, CP-3, and CP-4. The origin of the XYZ coordinate is located at CP-2. The location of the August 5, 1982, and June 29, 1982, data sets are indicated by the shaded areas.

Split the big cube into eight sub-cubes through the point p. V1 through V8 are volumes of sub-cube which correspond to Node 1 through Node 8 located diagonally from the volume element. (Such as the shady volume V1 corresponds to Node 1.) If a1 through a8 are the wind speed values on corresponding nodes, then the value of wind speed at point p is:

$$W_p = \frac{\sum_{i=1}^{8} W_i v_i}{\sum_{i=1}^{8} v_i}$$

Total Number of Data Values
= (81 x 81 x 9) x (3 wind components)
= (59049) x (3 wind components)
= 177147 data values

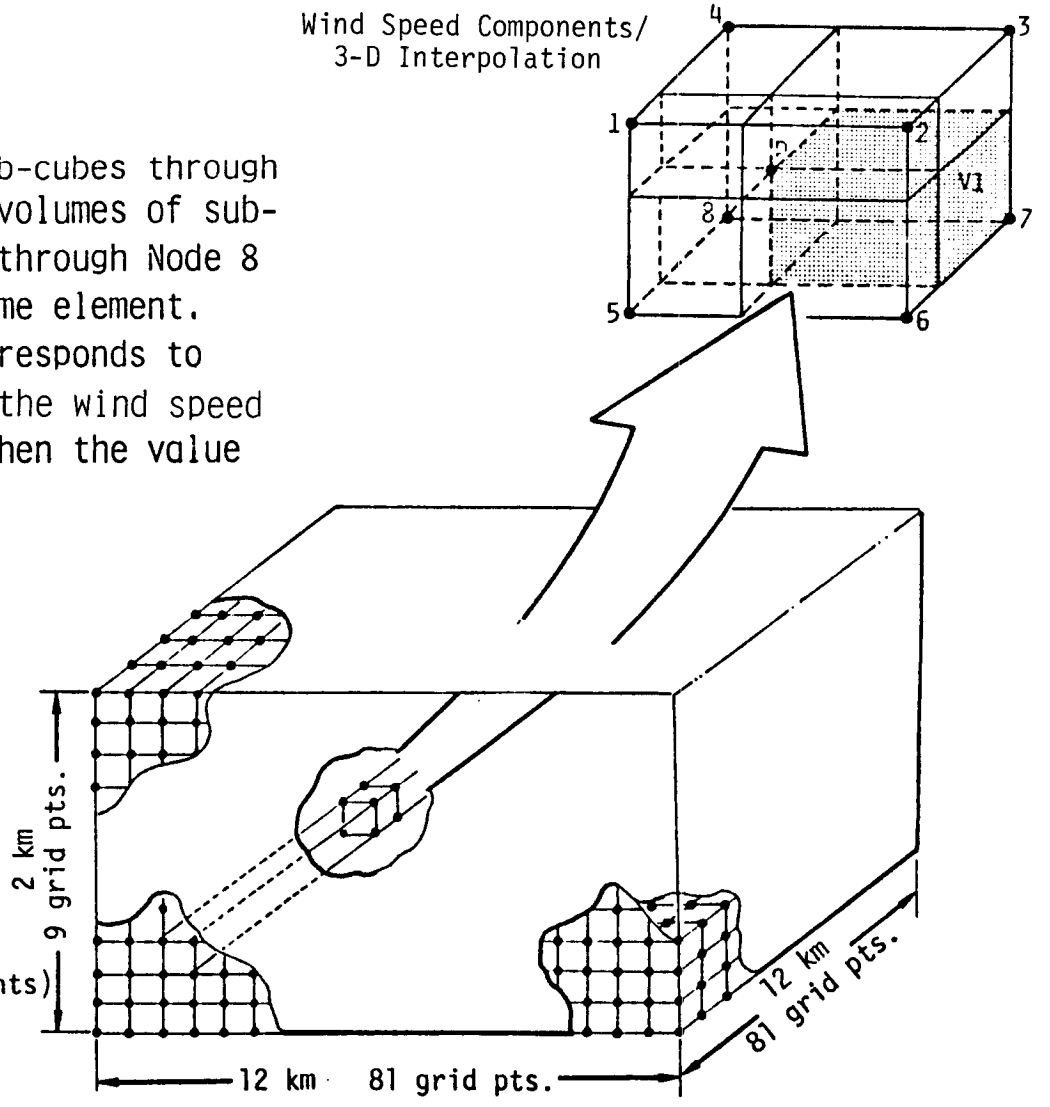

Figure 3. Handling the variable wind

a problem. However, I think this is not true for the NASA simulators. In turn, at FWG Associates we have had problems with our very small super micro-computer (40 kilobytes of storage) in storing that much data. Storage capacity on modern computers is not difficult to obtain. In the event that storage becomes a problem, we have selected volume elements of the data set, which I will describe to you in a moment.

Recall that we are also talking about turbulence parameters for each grid station, such as turbulence intensities and length scales, if we can extract these from the radar signals. In turn, if you are interested in heavy rain, we can provide radar reflectivity. Thus, there may be as many as six parameters for each grid point. The storage capacity is thus doubled. The question of whether we can handle storage capacities of these magnitudes is one of the issues we want to discuss. Another problem which was identified was not so much storage as interpolation to find the wind speeds at the aircraft position at 64 times per second. This, I believe, is the typical rate for most simulators. The procedure we currently use is a volume weighting procedure as illustrated in Figure 3. If the airplane is at point p, we simply weight velocity at a neighboring grid point with the diagonally opposite sub-volume element. Thus, we interpolate the winds at the point and when the airplane moves to the next point, we repeat the interpolation. This would seem to take considerable time on a computer, but actually this represents only about eight or nine lines of computer programming, and is not difficult to do (see ref. 3). Moreover, NASA is doing it in real time on their simulator. Thus, I believe, handling this large amount of data is not difficult, and the urgent need for a simple analytical model everyone is talking about is not that pressing. I firmly believe that simply storing the full volume data set is the simplest model you can get. By the time you come up with a model that is representative of true microburst wind shear, it is just as easy to use realistic data that have been measured in the field.

Now let me address another issue which I hope will be discussed in detail. I feel it is very important to put the spatial derivatives or wind gradient into the aircraft equations of motion. There are nine spatial gradients of winds (Figure 4). These have never really been considered in previous analyses of aircraft motion, partly because we did not have the information available. I will show you later that the gradients do enter the analysis, and in some cases, we think can be very significant. Therefore, in addition to interpolating for the three wind speed components, you must also interpolate for the wind gradients when using JAWS data sets. Again, this interpolation is not excessively time consuming (ref. 3).

In order to assist you, the user of the JAWS data sets, we have identified paths through the full volume set along which wind shears occur. We have classified these as to severe, moderate, and light wind shear. The paths were initially selected by inspection. Figure 5 is a plot of the horizontal winds at ground level. The vectors indicate the direction of the wind and the size of the vector indicates the magnitude. The center of the microburst is clearly visible. We picked flight paths where a strong head wind changed to a strong tail wind along the path. If, for example, you fly through this data base, say along YZ, you have a strong head wind shifting to a tail wind. We picked a number of paths just by inspection. The path IJ was selected because it is interesting in that a relatively strong lateral wind shear occurs. Also, we selected some paths such as GH that we knew were relatively benign, but still challenging. We analyzed the particular wind field by conducting a computer simulation of aircraft performance along the respective paths. The aircraft was trimmed for a 3° approach along this flight path. Simple control law algorithms were used to maintain the approach path. The runway can be moved relative to the wind, or the wind relative to the runway, whichever way you like to look at it. A 3° approach along flight path AB, for example, with the runway at any position

$$\begin{bmatrix} \frac{\partial W_x}{\partial x} & \frac{\partial W_x}{\partial y} & \frac{\partial W_x}{\partial z} \\ \frac{\partial W_y}{\partial x} & \frac{\partial W_y}{\partial y} & \frac{\partial W_y}{\partial z} \\ \frac{\partial W_z}{\partial x} & \frac{\partial W_z}{\partial y} & \frac{\partial W_z}{\partial z} \end{bmatrix}$$

Figure 4. Wind vector gradients appear in the governing equations of motion for the aircraft (nine derivatives)

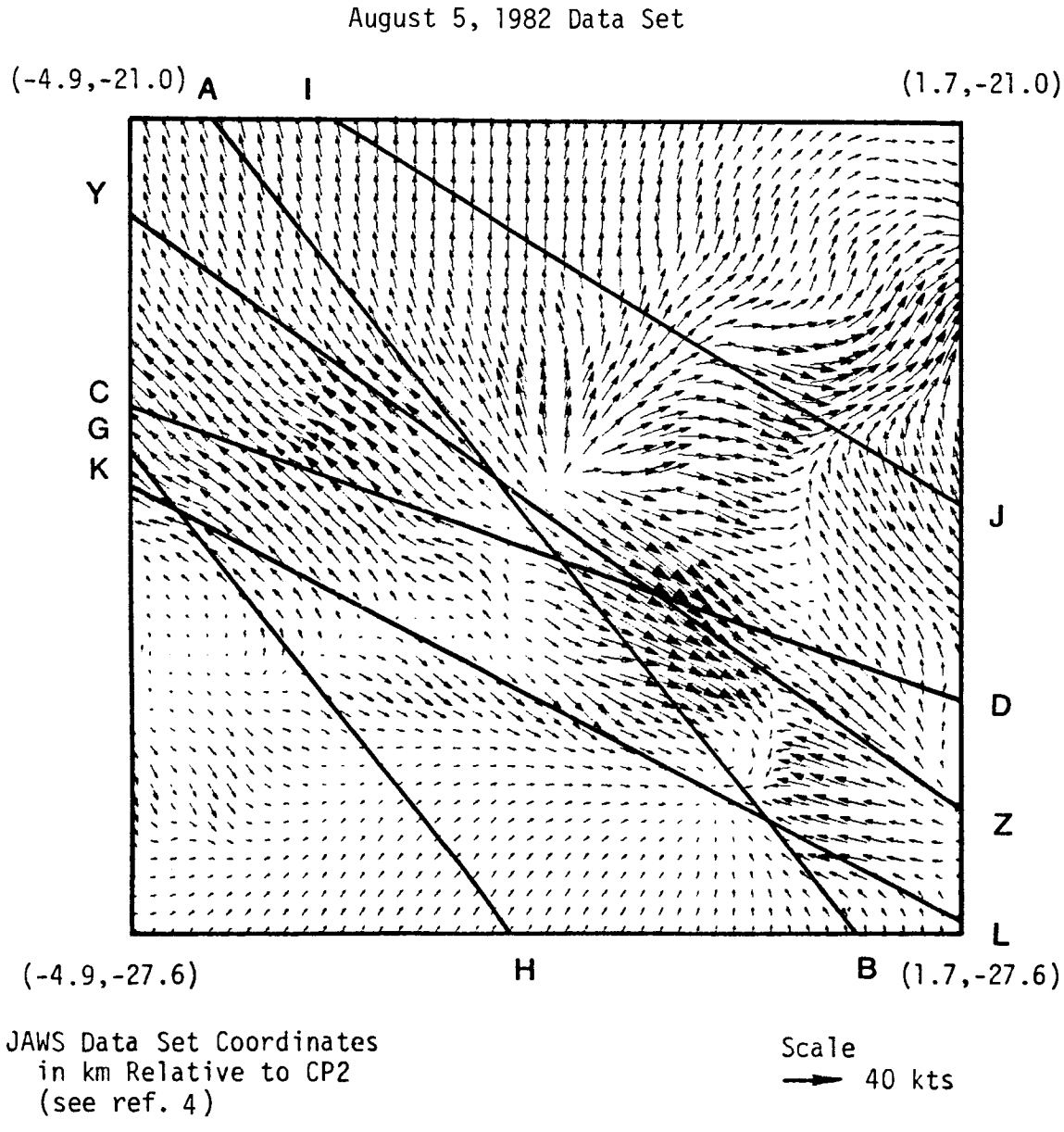

Figure 5. Flight paths overlaid on horizontal wind speed vectors

relative to where the center of the microburst is encountered can be simulated. We also simulated aircraft takeoff, with the position the aircraft flies through the microburst center again being adjusted. We ran several computer analyses and picked out what we classified as severe, moderate, and weak wind shear cases. The severe case on approach is one that our computer simulation, using relative simple control laws, was unable to fly; in other words, those cases in which the aircraft encountered the center of the microburst at a low altitude (roughly 100 m above the ground). In these cases, regardless of the fact that the control algorithm commands 15° to 20° pitch and full thrust to go-around, the aircraft could not fly and crashed; we called these cases moderate. We called those paths weak where a go-around was possible without too much difficulty, but where there was enough wind shear to make the control laws move around significantly.

A description of the paths and the nomenclature used to define them is shown in Figure 6. We trimmed the aircraft at roughly 2,000 ft. outside the data set. Then we picked some coordinates for each path which would represent the point at which the center of the microburst occurred. We measured those coordinates relative to the northwest corner of the data set. The coordinates of the NW corner shown on the figure are relative to CP-2. A new coordinate system for this specific data set is defined such that x_0 is the distance toward the east to the center of the microburst; y_0 is the distance toward the south to the center of the microburst, and z_0 is the height at which the airplane would pass through that microburst if it were able to maintain the 3° glide slope along the designated path. For example, taking line AB shown in Figure 5, the runway is oriented along this path and the aircraft is trimmed to make a 3° glide slope; x_0 and y_0 then indicate the position of the microburst center relative to the end of the runway, and z_0, which is a very critical parameter, is the height at which the airplane would pass through the microburst. The angle shown on Figure 6 is the angle of the path relative to the x_0 axis.

To reduce the magnitude of the data sets for the convenience of the user, we picked particluar flight paths, for example, path AB in Figure 5, and prepared sub-volume data sets called 1-, 2-, and 3-plane models. The sub-volume data sets were constructed by passing a vertical plane and two parallel planes on each side separated by 500 ft. through AB. Data from the full volume data set were then transformed to these data planes. The longitudinal velocity, w_x, relative to the plane is the wind speed component along the direction of the particular flight path (i.e., AB in this case), is the lateral wind which is perpendicular to x, and w_z is measured in the positive z direction upward.

The center of the microburst (or roughly the center) is the origin of the coordinate system. Figure 7 schematically illustrates how the data are tabulated on a corridor data set.

Figure 8 is a portion of a corridor data table for a 3-plane data set. A corridor along path AB is shown. The wind shear along this path is classified as severe, the origin is at the center of the microburst, the planes are separated by 500 ft. Plane 1 is 500 ft. to the side of the center plane and 3 is 500 ft. to the other side. Plane 2 runs directly down path AB (see Figure 5). The first column is the position along the path measured from the center of the microburst. The next three columns are the wind speed components in the x,y, and z direction, respectively. Notice that x is negative until the center of the microburst, i.e., x = 0. Then it is measured positive. To perform

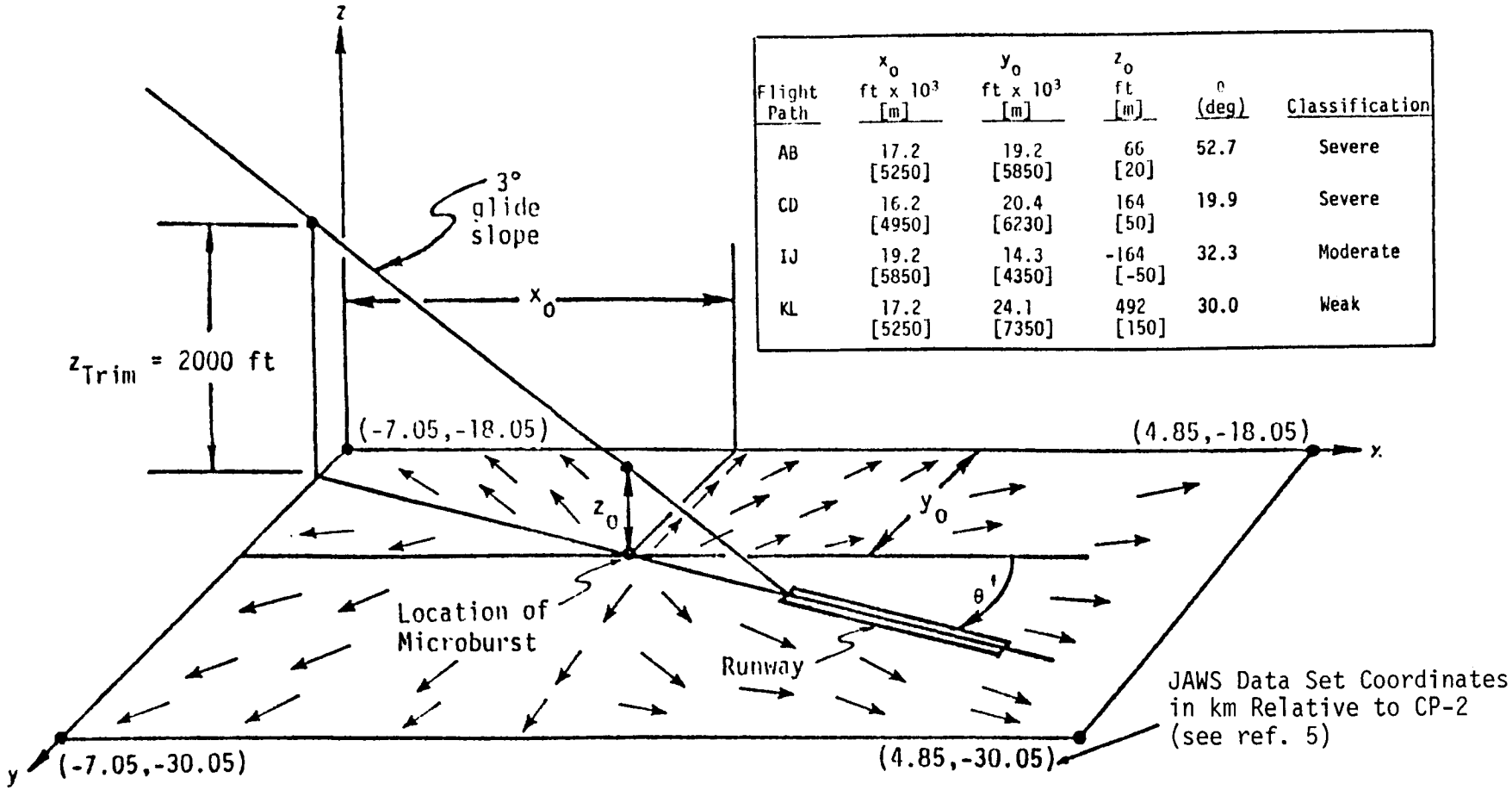

Flight Path	x_0 ft x 10^3 [m]	y_0 ft x 10^3 [m]	z_0 ft [m]	θ (deg)	Classification
AB	17.2 [5250]	19.2 [5850]	66 [20]	52.7	Severe
CD	16.2 [4950]	20.4 [6230]	164 [50]	19.9	Severe
IJ	19.2 [5850]	14.3 [4350]	-164 [-50]	32.3	Moderate
KL	17.2 [5250]	24.1 [7350]	492 [150]	30.0	Weak

Figure 6. Description of coordinate system and approach path orientation

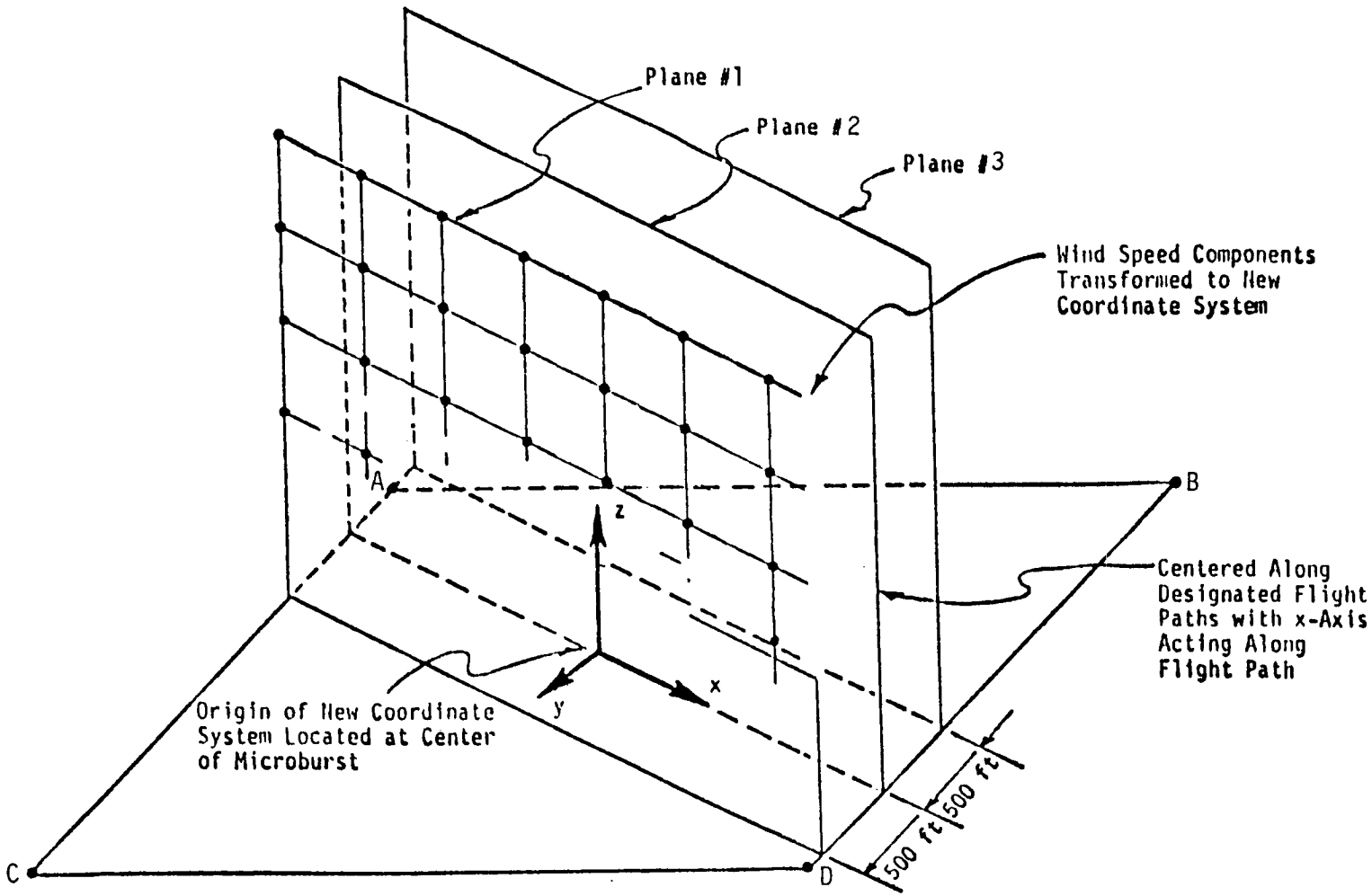

Figure 7. Description of coordinate system and data planes

JAWS WIND FIELD #1

(Corridor Along Path AB)

Profile Severity: Severe
Origin at Center of Microburst
Planes Separated by 500 ft

Elevation: 0 ft AGL

	PLANE 1			PLANE 2			PLANE 3		
X	Wx	Wy	Wz	Wx	Wy	Wz	Wx	Wy	Wz
-37500.	.00	.00	.00	.00	.00	.00	.00	.00	.00
-37000.	.00	.00	.00	.00	.00	.00	.00	.00	.00
-36500.	.00	.00	.00	.00	.00	.00	.00	.00	.00
-36000.	.00	.00	.00	.00	.00	.00	.00	.00	.00
-35500.	.00	.00	.00	.00	.00	.00	.00	.00	.00
-35000.	.00	.00	.00	.00	.00	.00	.00	.00	.00
-34500.	.00	.00	.00	.00	.00	.00	.00	.00	.00
-34000.	.00	.00	.00	.00	.00	.00	.00	.00	.00
-33500.	.00	.00	.00	.00	.00	.00	.00	.00	.00
-33000.	.00	.00	.00	.00	.00	.00	.00	.00	.00
-32500.	.00	.00	.00	.00	.00	.00	.00	.00	.00
-32000.	.00	.00	.00	.00	.00	.00	.00	.00	.00
-31500.	.00	.00	.00	.00	.00	.00	.00	.00	.00
-31000.	.00	.00	.00	.00	.00	.00	.00	.00	.00
-30500.	.00	.00	.00	.00	.00	.00	.00	.00	.00
-30000.	.00	.00	.00	.00	.00	.00	.00	.00	.00
-29500.	.00	.00	.00	.00	.00	.00	.00	.00	.00
-29000.	.00	.00	.00	.00	.00	.00	.00	.00	.00
-28500.	.00	.00	.00	.00	.00	.00	.00	.00	.00
-28000.	.00	.00	.00	.00	.00	.00	.00	.00	.00
-27500.	.00	.00	.00	.00	.00	.00	.00	.00	.00
-27000.	.00	.00	.00	.00	.00	.00	.00	.00	.00
-26500.	.00	.00	.00	.00	.00	.00	.00	.00	.00
-26000.	.00	.00	.00	.00	.00	.00	.00	.00	.00
-25500.	.00	.00	.00	.00	.00	.00	.00	.00	.00
-25000.	.00	.00	.00	.00	.00	.00	.00	.00	.00
-24500.	.00	.00	.00	.00	.00	.00	-7.72	2.60	.00
-24000.	.00	.00	.00	-7.75	2.79	.00	-7.74	2.42	.00
-23500.	-7.84	2.76	.00	-7.76	2.48	.00	-7.72	2.18	.00
-23000.	-7.90	2.18	.00	-7.77	2.15	.00	-7.66	1.93	.00
-22500.	-7.84	1.58	.00	-7.78	1.77	.00	-7.68	1.67	.00
-22000.	-7.60	1.38	.00	-7.47	1.32	.00	-7.44	1.30	.00
-21500.	-7.41	1.47	.00	-7.27	1.11	.00	-7.25	.81	.00
-21000.	-7.34	1.87	.00	-7.22	1.29	.00	-7.36	.95	.00
-20500.	-7.24	2.19	.00	-7.30	1.73	.00	-7.43	1.42	.00
-20000.	-7.16	2.21	.00	-6.97	1.83	.00	-7.09	1.66	.00
-19500.	-7.32	2.41	.00	-6.83	2.06	.00	-6.92	2.00	.00
-19000.	-7.74	3.31	.00	-7.55	3.05	.00	-7.54	3.00	.00
-18500.	-8.21	4.38	.00	-8.26	4.18	.00	-8.31	3.91	.00
-18000.	-8.56	5.44	.00	-8.67	4.74	.00	-8.74	4.00	.00
-17500.	-8.99	6.17	.00	-9.00	4.97	.00	-9.07	3.91	.00
-17000.	-9.58	6.48	.00	-9.60	5.39	.00	-9.42	4.17	.00
-16500.	-10.69	6.86	.00	-10.52	5.94	.00	-9.95	4.88	.00
-16000.	-11.69	7.28	.00	-11.61	6.45	.00	-10.91	5.48	.00
-15500.	-11.40	7.29	.00	-11.27	6.65	.00	-10.70	5.70	.00
-15000.	-11.33	7.10	.00	-10.36	6.56	.00	-9.64	5.70	.00
-14500.	-11.88	6.82	.00	-10.34	6.24	.00	-9.39	5.35	.00
-14000.	-12.54	6.60	.00	-11.14	5.91	.00	-10.00	4.95	.00
-13500.	-13.31	6.37	.00	-12.22	5.76	.00	-11.26	4.80	.00
-13000.	-13.81	5.73	.00	-13.48	5.54	.00	-12.27	4.62	.00
-12500.	-14.05	4.83	.00	-13.97	4.89	.00	-12.95	4.42	.00
-12000.	-13.83	4.30	.00	-13.74	4.70	.00	-12.75	4.51	.00
-11500.	-13.15	4.62	.00	-12.84	4.87	.00	-11.92	4.80	.00
-11000.	-12.00	4.92	.00	-11.76	4.97	.00	-11.22	4.81	.00
-10500.	-11.15	5.13	.00	-10.93	4.99	.00	-10.72	4.70	.00
-10000.	-10.50	5.17	.00	-10.41	4.96	.00	-10.33	4.70	.00
-9500.	-10.02	5.16	.00	-10.03	4.89	.00	-10.02	4.61	.00
-9000.	-9.66	5.09	.00	-9.75	4.79	.00	-9.80	4.50	.00
-8500.	-9.40	4.99	.00	-9.51	4.68	.00	-9.65	4.37	.00
-8000.	-9.22	4.88	.00	-9.35	4.55	.00	-9.50	4.22	.00

W_x = longitudinal wind; W_y = lateral wind; W_z = vertical wind
x = horizontal distance

JAWS WIND FIELD #1 (continued)

(Corridor Along Path AB)

Elevation: 0 ft AGL

-7500.	-9.14	4.76	.00	-9.32	4.41	.00	-9.60	4.02	.00
-7000.	-9.14	4.61	.00	-9.42	4.22	.00	-9.75	3.80	.00
-6500.	-9.24	4.43	.00	-9.64	4.00	.00	-10.04	3.53	.00
-6000.	-9.48	4.23	.00	-9.92	3.75	.00	-10.43	3.24	.00
-5500.	-9.83	4.02	.00	-10.31	3.49	.00	-10.97	2.90	.00
-5000.	-10.33	3.82	.00	-10.93	3.22	.00	-11.71	2.53	.00
-4500.	-10.95	3.62	.00	-11.78	2.93	.00	-12.79	2.14	.00
-4000.	-11.58	3.45	.00	-13.14	2.63	.00	-14.30	1.73	.00
-3500.	-13.21	3.27	.00	-14.92	2.32	.00	-15.89	1.21	.00
-3000.	-14.25	2.98	.00	-15.67	1.90	.00	-15.71	.65	.00
-2500.	-14.19	2.98	.00	-13.85	1.76	.00	-14.38	.38	.00
-2000.	-15.65	4.17	.00	-13.25	2.11	.00	-12.88	.33	.00
-1500.	-17.54	5.37	.00	-12.51	1.76	.00	-11.29	-.12	.00
-1000.	-16.15	5.29	.00	-11.90	1.57	.00	-9.20	-.63	.00
-500.	-15.42	5.40	.00	-11.80	1.74	.00	-9.95	-.03	.00
0.	-12.65	4.66	.00	-11.67	1.10	.00	-9.45	-.17	.00
500.	-4.24	3.23	.00	-4.23	.53	.00	-4.82	-.32	.00
1000.	7.19	2.92	.00	4.50	1.14	.00	2.62	.58	.00
1500.	13.40	3.79	.00	11.03	2.71	.00	8.33	2.11	.00
2000.	17.74	5.25	.00	15.19	4.77	.00	12.55	4.68	.00
2500.	22.02	7.91	.00	18.75	7.95	.00	15.85	7.06	.00
3000.	27.12	9.74	.00	21.78	10.10	.00	17.68	8.51	.00
3500.	30.67	10.04	.00	22.98	9.77	.00	18.51	8.38	.00
4000.	27.83	9.11	.00	22.32	9.00	.00	18.59	7.77	.00
4500.	25.39	8.12	.00	22.02	8.47	.00	19.78	7.93	.00
5000.	25.31	8.19	.00	24.36	9.32	.00	21.29	9.86	.00
5500.	24.18	9.13	.00	25.07	11.51	.00	22.38	12.22	.00
6000.	23.06	9.93	.00	23.88	12.12	.00	21.67	12.99	.00
6500.	22.81	9.18	.00	23.56	10.42	.00	21.24	10.99	.00
7000.	22.12	7.35	.00	21.24	7.77	.00	18.76	7.29	.00
7500.	17.35	5.26	.00	15.81	5.40	.00	13.06	5.19	.00
8000.	11.22	3.86	.00	7.58	3.51	.00	8.04	3.59	.00
8500.	6.85	1.42	.00	4.69	1.64	.00	4.27	1.83	.00
9000.	5.13	-.53	.00	2.47	-.32	.00	1.31	-.09	.00
9500.	3.70	-3.10	.00	2.18	-2.50	.00	-1.26	-2.49	.00
10000.	1.68	-5.01	.00	1.06	-3.97	.00	-1.90	-3.54	.00
10500.	-3.71	-6.80	.00	-1.85	-4.04	.00	-2.62	-2.90	.00
11000.	-9.04	-8.38	.00	-5.66	-4.82	.00	-4.06	-2.43	.00
11500.	-11.47	-9.00	.00	-7.50	-5.11	.00	-5.33	-2.55	.00
12000.	-11.42	-8.52	.00	-8.21	-5.12	.00	-6.11	-2.55	.00
12500.	-11.37	-8.79	.00	-8.66	-5.47	.00	-6.53	-2.50	.00
13000.	-11.51	-9.64	.00	-9.13	-6.49	.00	-6.71	-2.41	.00
13500.	-10.50	-8.57	.00	-8.35	-5.14	.00	-6.54	-1.93	.00
14000.	-7.97	-4.59	.00	-6.75	-2.33	.00	-5.71	-.37	.00
14500.	-5.88	-1.20	.00	-5.36	-.05	.00	-5.01	.81	.00
15000.	-4.94	.47	.00	-4.67	1.13	.00	-4.49	1.74	.00
15500.	-4.47	1.52	.00	-4.28	2.02	.00	-4.17	2.43	.00
16000.	-4.20	2.29	.00	-4.11	2.64	.00	-4.00	2.95	.00
16500.	-4.04	2.86	.00	-4.01	3.12	.00	-3.95	3.38	.00
17000.	-3.94	3.25	.00	-3.94	3.50	.00	-3.93	3.73	.00
17500.	-3.90	3.56	.00	-3.91	3.76	.00	-3.93	3.97	.00
18000.	-3.90	3.80	.00	-3.91	3.95	.00	-3.92	4.11	.00
18500.	-3.90	3.97	.00	-3.91	4.09	.00	-3.90	4.22	.00
19000.	-3.89	4.12	.00	-3.89	4.22	.00	-3.87	4.34	.00
19500.	-3.86	4.27	.00	-3.84	4.34	.00	-3.82	4.45	.00
20000.	-3.75	4.43	.00	-3.76	4.49	.00	-3.75	4.58	.00
20500.	-3.61	4.59	.00	-3.65	4.66	.00	-3.65	4.74	.00
21000.	-3.49	4.77	.00	-3.47	4.86	.00	-3.49	4.94	.00
21500.	-3.26	4.96	.00	-3.22	5.08	.00	-3.20	5.18	.00
22000.	-2.82	5.17	.00	-2.76	5.36	.00	-2.70	5.44	.00
22500.	-1.60	5.38	.00	-1.43	5.63	.00	-1.62	5.67	.00
23000.	.16	5.34	.00	.29	5.84	.00	-.12	6.11	.00
23500.	.63	5.17	.00	.94	6.23	.00	.32	7.36	.00
24000.	-.23	5.56	.00	-.74	6.76	.00	-2.32	8.44	.00
24500.	-2.16	6.16	.00	-3.80	7.80	.00	-5.60	8.93	.00
25000.	-3.53	6.70	.00	-5.56	7.35	.00	.00	.00	.00
25500.	-3.58	6.82	.00	.00	.00	.00	.00	.00	.00

W_x = longitudinal wind; W_y = lateral wind; W_z = vertical wind
x = horizontal distance

Figure 8. Illustration of tabulated 3 planar data.

a simulation, the runway can be moved back and forth along the path and either takeoffs or landings can be simulated at any position relative to the center of the microburst

The important parameters, in terms of assuring that spatial wind shear is incorporated into the aircraft equations of motion, are $\dot{\alpha}$ and $\dot{\beta}$ and angular rotation. If the equations are written in the inertial coordinate system, then spatial derivatives appear in the equations of motion only in the aerodynamics coefficients (Figure 9), in the $\dot{\alpha}$ and $\dot{\beta}$ values, and in the angular rotations. Consider the $\dot{\alpha}$ and $\dot{\beta}$ terms as shown in Figure 10. Normally the derivative of alpha is taken to provide $\dot{\alpha}$ as shown in the figure. The values u and w are relative velocity values. Beta is handled similarly. To obtain the derivatives of the velocity, you write the equations in the body coordinate system and solve for $\dot{u}$ and $\dot{w}$ (see Figure 10). Notice that $\dot{u}$ and $\dot{w}$ contain spatial derivatives of the wind. Thus when computing $\dot{\alpha}$, the spatial derivatives automatically appear in your equations of motion. Remember that W_X, W_Y, and W_Z are given in earth coordinates and must be transformed to the body coordinates.

The spatial wind derivatives become even more important in their effect on rotations which appear in the aerodynamic coefficients (see Figure 9). For example, the lift coefficients, as aerodynamic derivatives with respect to p and q, are with respect to relative rotation. What is typically done in most systems of equations of motion is to solve for inertial values. Moment equations are typically formulated in an inertial coordinate system. What happens, however, is that the airplane is rotating relative to the earth (the normally computed rotation values), but the wind is also rotating (see Figure 11). The JAWS data show there is a lot of rotation in the wind (see Figure 12); therefore, the rotation of the wind must be subtracted from the inertial rotation of the airplane to get the relative rotation. The rotation of the wind comes directly from the nine derivatives, because angular rotation of the atmosphere is the anti-symmetric part of the tensor gradient (see Figure 13). The equations for the rotation of the aircraft relative to the airmass are given in Figure 13. The inertial values calculated from the moment equation are reduced by the angular rotation of the wind and appropriately transformed into the body coordinate system. These resulting values should be used to calculate the aerodynamic coefficients. We believe that these terms are fairly significant.

Details of the wind shear models are given in reference 5 and of the aircraft equations of motion in reference 6. Standardization of the procedure for implementing wind shear into simulators is imperative if meaningful training and exchange of results are to be achieved.

Lift Force:

$$L = C_L \rho V^2 A/2$$

$$C_L = C_{L_0} + C_{L_\alpha}(\alpha) + C_{L_{\delta_E}}(\delta_E) + \frac{\bar{C}}{2V}(C_{L_q}(q) + C_{L_{\dot{\alpha}}}(\dot{\alpha}))$$

$$+ \text{ground effect}$$

Drag Force:

$$D = C_D \rho V^2 A/2$$

$$C_D = C_{D_0} + C_{D_\alpha}(\alpha) + C_{D_R}(\theta_R) + C_{D_\beta}(\beta) + \text{ground effect}$$

where

C_{D_R} = drag coefficient due to rudder

C_{D_β} = drag coefficient due to side-slip

Moment:

$$M = C_M \rho V^2 \bar{C}/2$$

$$C_M = C_{M_0} + C_{M_\alpha}(\alpha) + C_{M_{\delta_E}}(\delta_E) + \frac{\bar{C}}{2V}(C_{M_q}(q) + C_{M_{\dot{\alpha}}}(\dot{\alpha}))$$

$$+ C_{M_R}(\theta_R) + C_{M_\beta}(\beta) + \text{engine thrust effect}$$

$$+ \text{ground effect}$$

where

C_{M_R} = change pitch due to rudder

C_{M_β} = change pitch due to side-slip

Figure 9. Lift, drag, and moment coefficients

$$\alpha = \frac{w}{u} \; ; \quad \dot{\alpha} = \frac{u\dot{w} - w\dot{u}}{u^2 + w^2}$$

$$\beta = \frac{v}{V} \; ; \quad \dot{\beta} = \frac{\dot{v}(u^2 + w^2) - v(u\dot{u} + w\dot{w})}{V^2\sqrt{u^2 + w^2}}$$

where

$$\dot{u} = \frac{X}{m} - g \sin\theta - \dot{W}_x - [q(w + W_z) - r(v + W_y)]$$

$$\dot{v} = \frac{Y}{m} + g \cos\theta \sin\phi - \dot{W}_y - [r(u + W_x) - p(w + W_z)]$$

$$\dot{w} = \frac{Z}{m} + g \cos\theta \cos\phi - \dot{W}_z - [p(v + W_y) - q(u + W_x)]$$

Figure 10. Derivatives of α and β in body coordinates

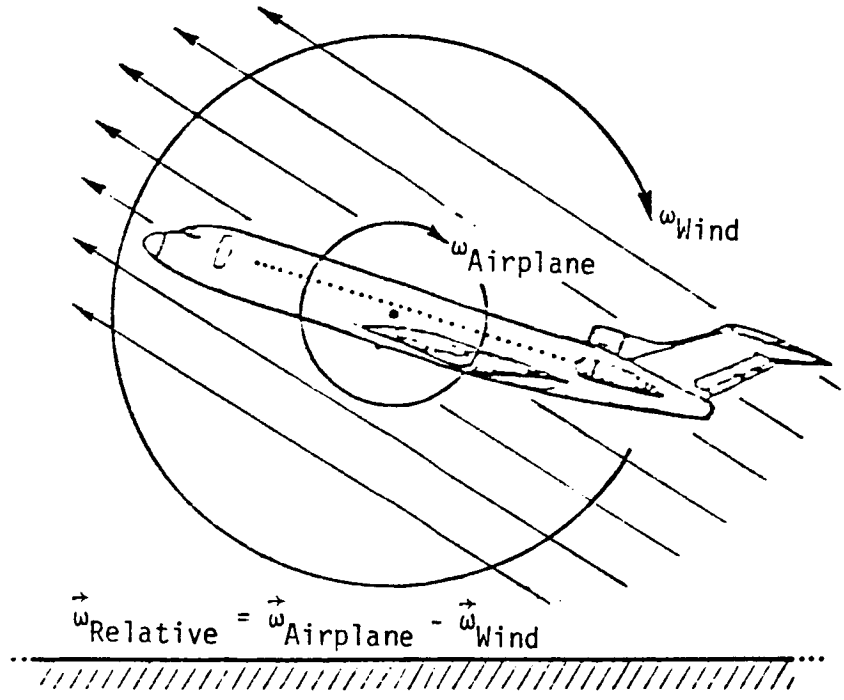

Figure 11. Schematic illustration of wind field rotation

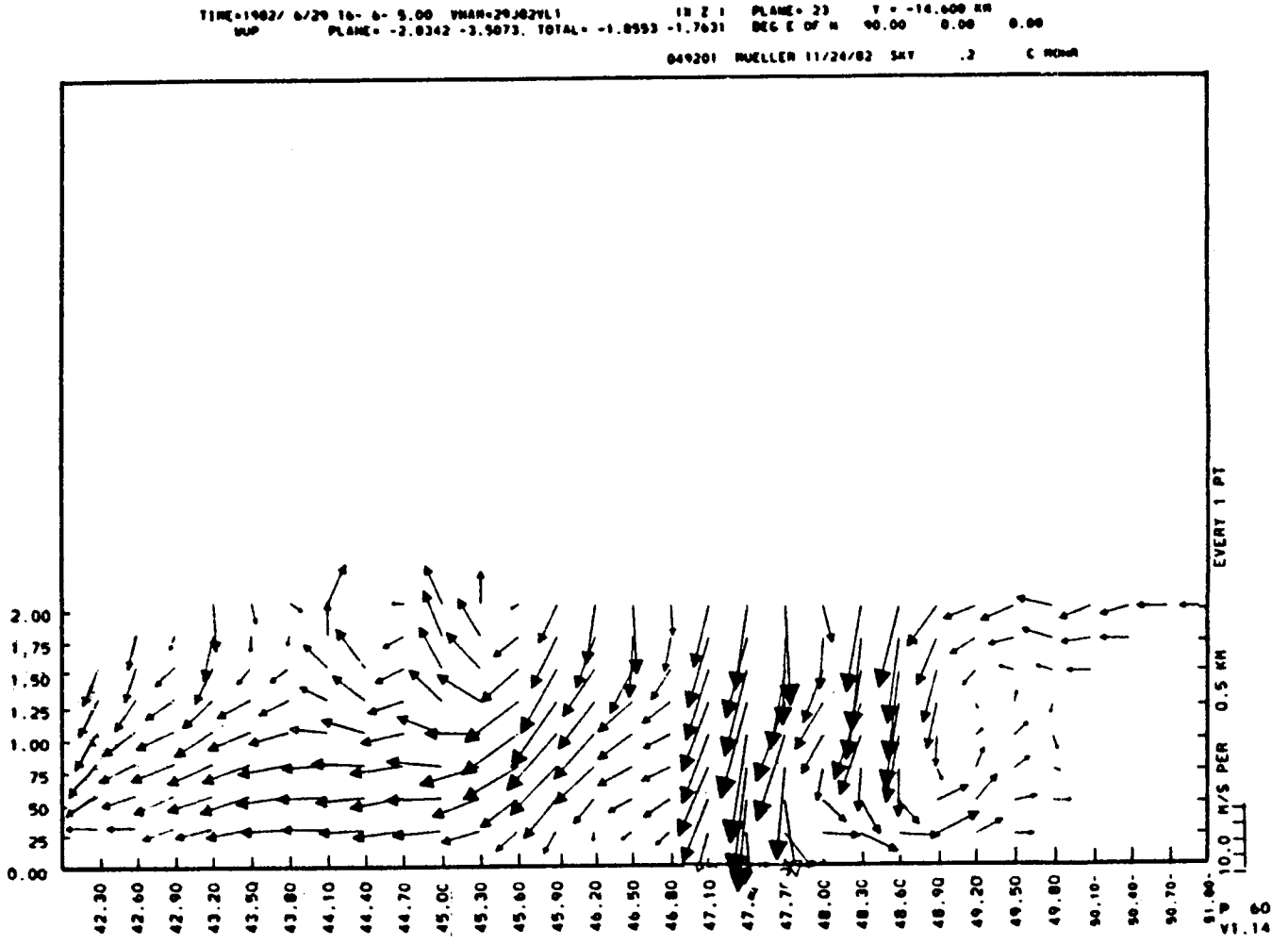

Figure 12. Shows rotation of wind field from JAWS data

- Relative angular rotation vector:

$$\vec{\omega}_{rel} = \vec{\omega} - \vec{\omega}_W$$

- Angular rotation of atmosphere (antisymmetric part of tensor gradient $\vec{\nabla}\vec{W}$):

$$\vec{\omega}_W = \frac{1}{2}\vec{\nabla} \times \vec{W}$$

  - Inertial coordinates:

$$\vec{\omega}_W = \frac{1}{2}\left(\frac{\partial W_z}{\partial y} - \frac{\partial W_y}{\partial z}\right)_E \vec{i} + \frac{1}{2}\left(\frac{\partial W_x}{\partial z} - \frac{\partial W_z}{\partial x}\right)_E \vec{j} + \frac{1}{2}\left(\frac{\partial W_y}{\partial x} - \frac{\partial W_x}{\partial y}\right)_E \vec{k}$$

  - Body coordinates:

$$\begin{bmatrix} p_{rel} \\ q_{rel} \\ r_{rel} \end{bmatrix} = \begin{bmatrix} p \\ q \\ r \end{bmatrix} - L_{BE} \begin{bmatrix} \left(\frac{\partial W_z}{\partial y} - \frac{\partial W_y}{\partial z}\right)_E \\ \left(\frac{\partial W_x}{\partial z} - \frac{\partial W_z}{\partial x}\right)_E \\ \left(\frac{\partial W_y}{\partial x} - \frac{\partial W_x}{\partial y}\right)_E \end{bmatrix}$$

Figure 13. Angular rotation relative to atmosphere

REFERENCES

1. Elmore, Kim: JAWS multiple Doppler derived winds. Wind Shear/Turbulence Inputs to Flight Simulation and Systems Certification, NASA CP-2474, 1987, pp. 29-42.

2. McCarthy, John: Status of the JAWS program. Wind Shear/Turbulence Inputs to Flight Simulation and Systems Certification, NASA CP-2474, 1987, 43-48.

3. Bowles, Roland: Wind shear and turbulence simulation. Wind Shear/Turbulence Inputs to Flight Simulation and Systems Certification, NASA CP-2474, 1987, pp. 67-96.

4. JAWS Project Operations Summary 1982. National Center for Atmospheric Research, Boulder, CO, 1983.

5. Frost, W.; Chang, H. P.; Elmore, K. L.; and McCarthy, J.: Simulated Flight Through JAWS Wind Shear: In-Depth Analysis Results. Journal of Aircraft, Volume 21, Number 10, 1984, pp. 797-802.

6. Frost, Walter; and Bowles, Roland L.: Wind shear terms in the equations of aircraft motion. Journal of Aircraft, Volume 21, Number 11, December 1984, p. 866.